JOURNAL OF MATERIALS SCIENCE 23 (1988) 3756–3763

Electromagnetic stirring of aluminium–silicon alloys

D. A. CURREY
Dofasco, P.O. Box 460, Hamilton, Ontario, L8N 3J5, Canada

C. A. PICKLES
Department of Metallurgical Engineering, Queen's University, Kingston, Ontario, K7L 3N6 Canada

A laboratory-scale electromagnetic stirrer was designed, constructed and tested on two aluminium–silicon alloys with silicon contents of seven and twenty mass per cent. The effect of stirring intensity on the structure of the hypoeutectic alloy was studied and also thermal analysis was performed. For the case of the hypereutectic alloy, the distribution of silicon was determined. The results demonstrate that electromagnetic stirring reduced the amount of silicon segregation in the hypereutectic alloy, while in the hypoeutectic alloy stirring promoted dendrite fragmentation. In addition, the axial porosity was reduced and the core of the ingot was more sound. Electromagnetic stirring affects the solidification process by the stirring action and also by extending the time of thermal arrest.

1. Introduction

High strengths in metals can be achieved through the development of a microstructure consisting of fine grains, which have a narrow size distribution. Further improvements are possible by minimizing both anisotropy and segregation effects which develop during solidification. One method of affecting the solidification process is by electromagnetic stirring of the melt during solidification. This reduces the temperature and compositional gradients in the melt and thus promotes a uniform structure throughout the casting. The magnitude of the effects of stirring are related to the fluid and heat flow conditions which are established in the melt.

The fluid flow created by the stirring action results in grain multiplication. There are a number of mechanisms which have been proposed to explain this phenomenon. Firstly, the stirring action can feed the interdendritic spaces with fresh hot liquid which can result in melting and separation of the dendrite arms [1]. Secondly, if the flow velocities are over $0.25\,cm\,sec^{-1}$ then the adiabatic heat generated by this stress could be responsible for melting [2]. Also, under turbulent conditions, fatigue can cause the dendrite arms to separate [2].

Convection has been shown to have a significant effect on both grain size [3] and segregation [4] in a casting. Liquid penetration into the interdendritic regions during solidification is, to a large degree, a function of the convective forces. Forced convection can be employed to promote dendrite fragmentation and to increase the proportion of equiaxed grains.

The effects of electromagnetic fields on the solidification of aluminium alloys have been studied by a number of authors. Japanese workers employed unstable electromagnetically induced fluid oscillations to produce fine grained aluminium alloys [5, 6]. Russian researchers observed similar effects when aluminium alloys were cast into electromagnetic moulds [7]. More recently, Reddy and Sekhar studied the effect of forced convection on the structure of an Al–4.4 mass % Cu alloy [8]. It was found that both the grain size and the dendrite arm spacings were reduced. The reduction in dendrite arm spacing was attributed to the improved heat transfer rates between the casting and the mould wall.

In this work, a laboratory-scale linear electromagnetic stirrer was employed to study the effect of electromagnetic stirring on aluminium–silicon alloys. Linear stirrers can be used to reverse the normal convective flow patterns in a casting by producing fluid flow parallel to the vertical walls of the mould. The fluid motion created by this type of stirrer tends to contain the liquid rather than forcing it against the solid shell. Liquid from the top of the pool is transported to the bottom, helping to improve heat transfer and liquid mixing during solidification. With this equipment it was possible to study, under controlled conditions, the effects of casting and stirring parameters on the solidified product. Two aluminium–silicon alloys, with silicon contents of 7 and 20 mass %, were cast in the stirrer. The aluminium–silicon phase diagram is shown in Fig. 1. The hypereutectic alloy produces dendritic growth during solidification, allowing the effect of EMS on dendrite morphology to be studied. The hypereutetic alloy produces a dispersion of primary silicon precipitates, in the size range of 50–300 μm. Thus, in this alloy, the effect of stirring on the segregation of these precipitates could be evaluated.

0022–2461/88 $03.00 + .12

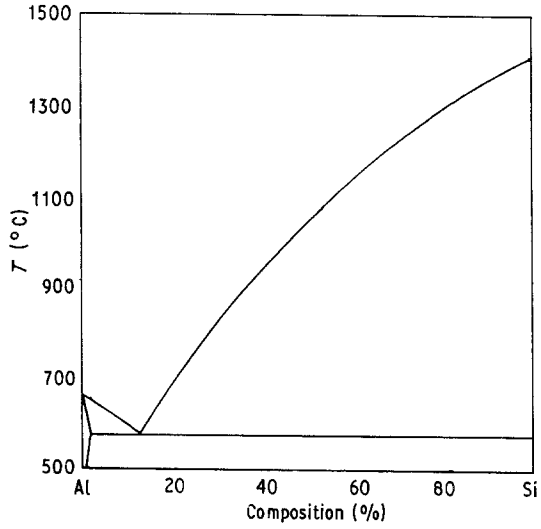

Figure 1 Aluminium–silicon phase diagram.

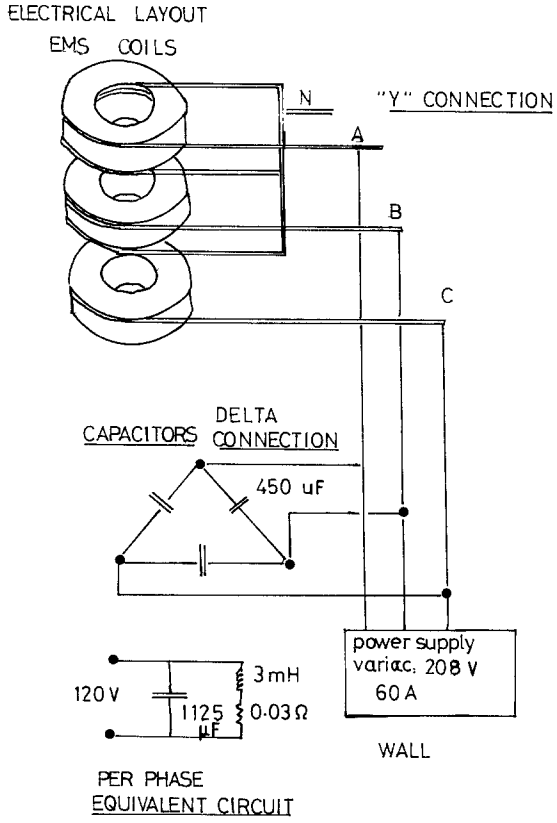

Figure 2 Schematic diagram of the electromagnetic stirrer unit.

2. Experimental aspects

A schematic diagram of the experimental apparatus is shown in Fig. 2. The linear EMS unit employed a 220 V, three-phase power supply at an operating frequency of 60 Hz, with a maximum current draw of 50 A. The unit was designed to produce a travelling wave with up to a 0.5 T magnetic field in the centre of the stirrer's three coils. The bore of the stirrer had a cylindrical cross-section with a diameter of 12.7 cm and an overall height of 47.0 cm. The unit was enclosed in a stainless steel container with a 1.3 cm layer of Microtherm powder insulation. Each of the three coils consisted of 72 turns of 0.48 cm in diameter copper tubing, which was used for water cooling and electrical transmission. The tubing was wrapped in thermal insulating tape and the finished coils were set in a polyester epoxy resin. Three sides of the stirrer were fitted with 14 gauge expanded metal covers which allowed air circulation around the coils. The remaining side had a removable aluminium cover, which permitted access to the electrical terminals, water cooling connections and insulating links. The top and bottom of the stirrer were fitted with aluminium covers. Also, the top was thermally insulated with a 1.3 cm layer of Microtherm insulation.

The power of the electromagnetic stirrer was measured using the instrumentation circuit diagram shown in Fig. 3. The magnetic field strength was measured with a flux probe constructed from 150 turns of No. 34 AWG enamelled copper wire wound on a 5 mm diameter glass rod. The wire was soldered onto a shielded extension cable and conncected to a double-beam oscilloscope. Measurements were taken

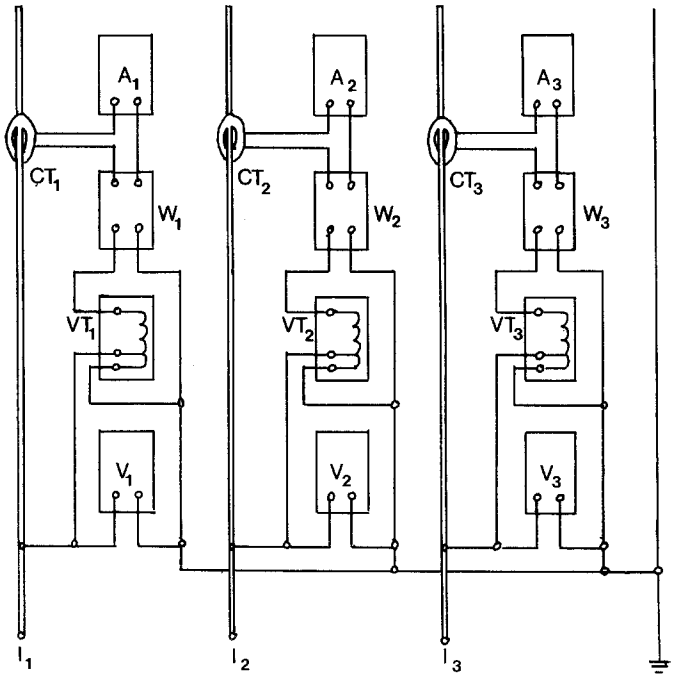

Figure 3 The electrical instrumentation circuit diagram employed for the magnetic field strength measurements.

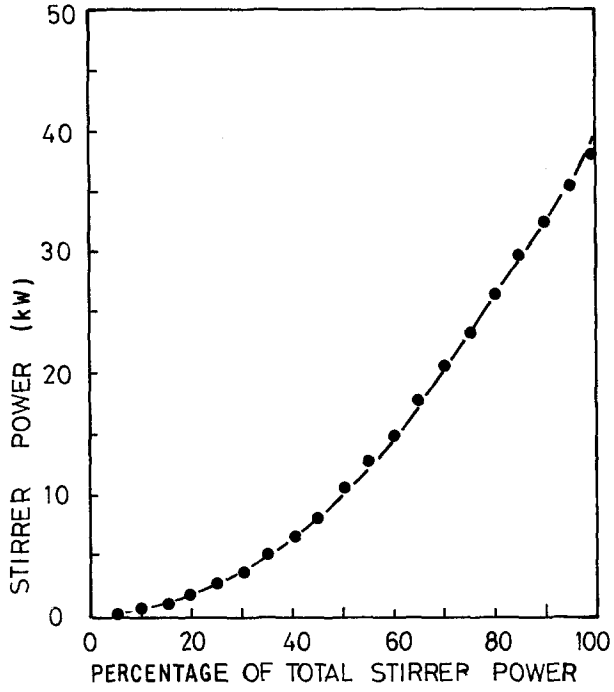

Figure 4 The variation of actual stirrer power with the percentage of maximum power.

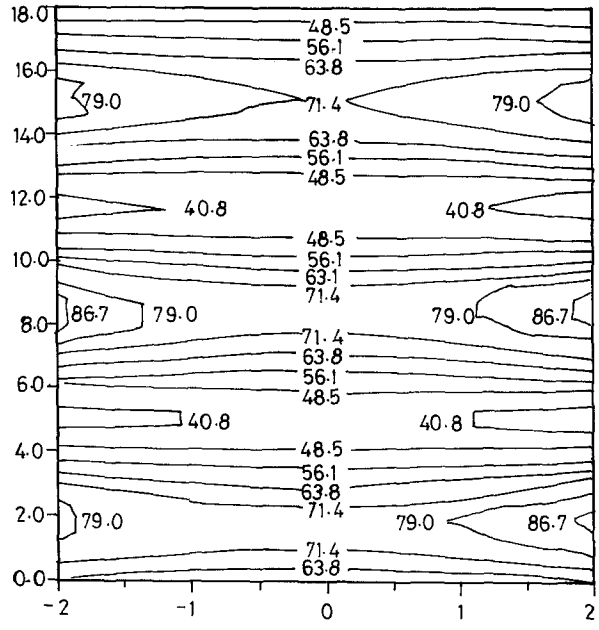

Figure 5 Contour map detailing the transverse profile of magnetic field strength across the bore of the stirrer. Data plotted from flux probe measurements taken with a total machine current of 50.3 A or 50% of maximum power.

across the transverse profile of the bore of the stirrer at 1.3 cm intervals. Readings were taken along the entire length of the stirrer, requiring a total of more than 300 measurements.

The two aluminium–silicon alloys used in this study were as follows

(1) Hypoeutectic alloy (7 mass % Si).

(2) Hypereutectic alloy (20 mass % Si).

The base alloy was a commercial purity aluminium–silicon alloy containing 7 mass % Si. High purity (98% pure) crystalline silicon was added to the base alloy to produce a hypereutectic alloy with 20 mass % Si. Alloys were preweighed and placed in an alumina-washed graphite crucible. The crucible was then heated in an induction furnace. After melting, a 15 min holding time was used to allow the melt to reach the required temperature of 850° C and to ensure a uniform temperature distribution throughout.

In order to study the effects of EMS on solidification, the contents of the crucible were poured with a superheat of 100° C into a mould positioned in the core of the stirrer. The mould used was a cylindrical, non-magnetic stainless steel crucible lined with a thermal setting resin sand. A new liner was used for each run. After cooling, the cast ingots were sectioned along the longitudinal axis. The surface was prepared by grinding and then etched for 10–12 min using 0.5 vol % hydrofluoric acid. This technique reveals the macrostructure, porosity, and silicon distribution in the casting.

Quantitative chemical analysis of the silicon distribution in the hypereutectic alloy ingots was determined by atomic absorption analysis. Drillings were taken across the ingot along the transverse axis at 8.4 mm intervals. The data was used to obtain the silicon concentration profiles at distances of 50 and 100 mm from the base of the casting. Additional samples were taken along the ingot centreline at 25 mm intervals. Approximately 0.1 g of each sample was dissolved in 10 ml of 50 vol % hydrochloric acid solution and allowed to cool to room temperature for 30 min. The solution was diluted to 100 ml with distilled water in a volumetric flask. After allowing the siliceous residue to settle, 10 ml of solution was pipetted into another volumetric flask. This final solution was made up to 100 ml with a solution containing 1 vol % hydrochloric acid and 0.1 vol % potassium chloride, with the balance being distilled water.

Samples were analysed for aluminium concentration using a Perkin-Elmer atomic absorption analyser with a wavelength of 309.3 nm and a slit of 0.7 nm. A nitrous oxide acetylene flame was employed and a linear calibration was obtained. The instrument was calibrated using aluminium standards of 50, 70 and 100 p.p.m. An average of three readings were taken at 2 sec intervals to determine the relative silicon concentration by difference in each sample. In order to confirm that the residue did not contain any aluminium, four identical samples were prepared to check the reproducibility of the analysis. The four separate solutions were tested for aluminium concentration using the atomic absorption technique described above.

The remaining solution was vacuum-filtered through a No. 42 filter paper. The residue was thoroughly washed with distilled water to remove any of the original solution containing dissolved aluminium. The filter papers were dried at room temperature and then placed in a covered ceramic crucible. The crucible was heated to 621° C in a muffle furnace for two hours to completely ignite the filter paper. After cooling, the residue was spread on a glass slide and qualitatively analysed using X-ray diffraction. The sample was exposed to molybdenum K-alpha radiation with a wavelength of 0.0710 nm. The only significant peaks observed corresponded to those for

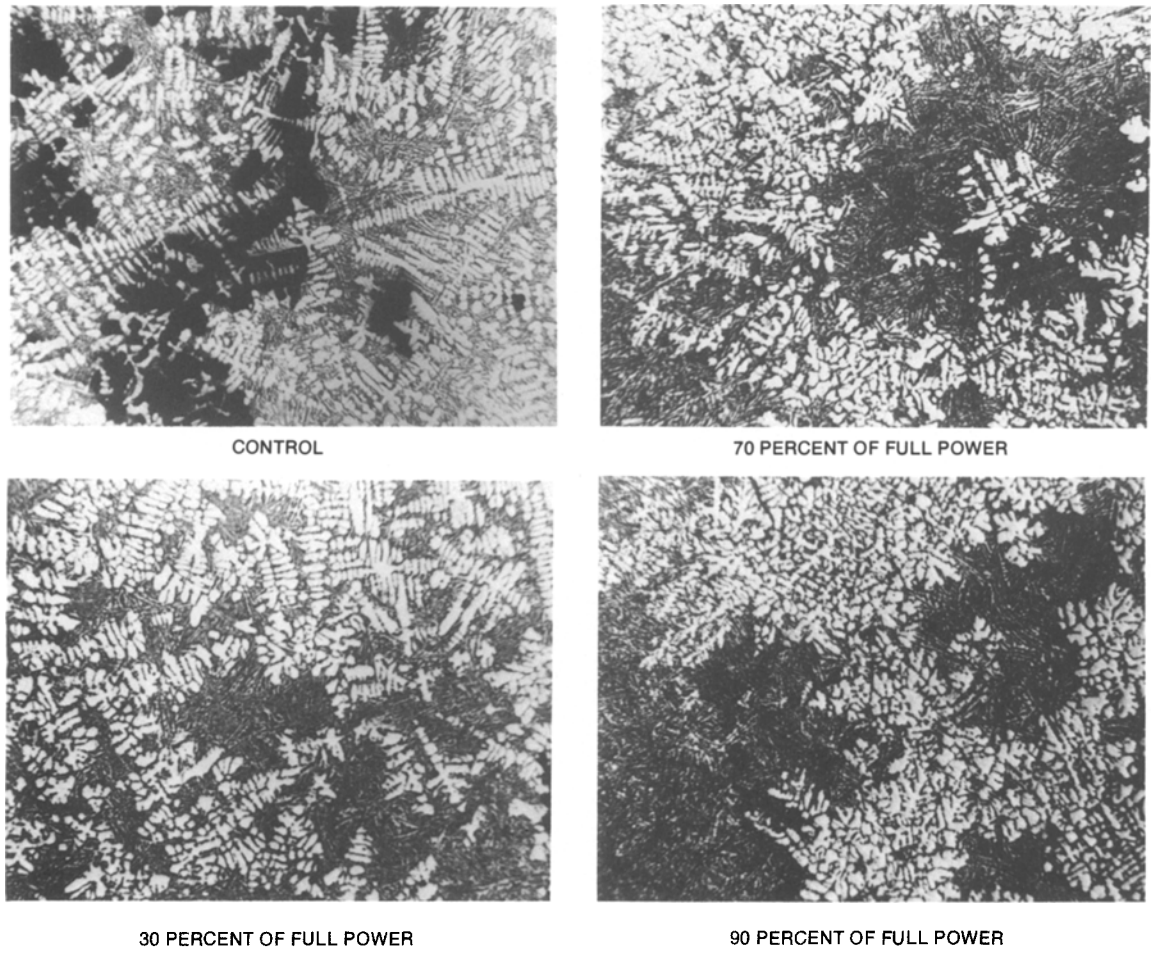

Figure 6 Photomicrographs detailing the effect of EMS on the morphology of the primary aluminium dendrites in the hypoeutectic Al–Si alloy.

pure crystalline silicon, indicating that no significant amount of aluminium was present. These results demonstrate that, in the dissolution step, the aluminium is completely dissolved and the residue is pure silicon.

Thermal analysis of ingot solidification was performed using chromel–alumel thermocouples. The tips of the couples were welded to ensure good electrical contact and were coated with a thin layer of alumina to prevent dissolution in the melt. Runs employing three thermocouples were conducted with the couples located near the mid-radius of the ingot, equidistant from the ingot centreline to minimize any localized interference effects. The couples were positioned to measure temperature changes at 4, 8, and 12 cm from the base of the 16 cm high ingots. Tests were also conducted with a single thermocouple positioned at the mid-radius which was 8 cm from the bottom of the melt.

In one series of tests a graphite paddle was placed in the centre of the melt. The purpose of these trials was to compare the effect of mechanical stirring with the graphite paddle at 100 r.p.m. for 15 min and electromagnetic stirring at 50% of full power for 15 min with normal solidification. The mechanical stirring rate was in excess of that obtained with EMS. The paddle was constructed from a cylindrical graphite rod 2 cm in diameter and 11.5 cm in length, with a 0.5 × 1.5 × 4.0 cm^3 paddle. The paddle was held in place by a graphite pin and a 0.64 cm diameter carbon steel rod was used for the support shaft. The pouring temperature of the melt was raised to 925° C to compensate for the presence of the graphite paddle, which would otherwise have acted as a heat sink, causing the melt to cool at a faster rate. Thermal analysis data was collected using a multi-channel stripchart recorder in the range of 20 to 30 mV.

3. Results and discussion

3.1. EMS operating characteristics

Fig. 4 shows the power curve for the EMS unit which indicates the actual stirrer power as a function of the power supplied to the stirrer (maximum power). It can be seen that in order to achieve significant stirrer power it is necessary to operate at over 30 to 40% of the total stirrer power. Fig. 5 is a contour map which details the transverse profile of the magnetic field across the bore of the linear electromagnetic stirrer. The map illustrates the flux patterns created by each of the three coils, as well as the interference effects between adjacent coils. The diagram demonstrates how the field diminishes with increasing distance from the inner radius of the coils. Additional losses would occur as the field passes through the solid shell of a solidifying ingot. As a result, large amounts of power are required to penetrate and stir the melt, particularly during the final stages of solidification.

3.2. Studies of hypoeutectic aluminium–silicon alloy solidification

The effect of stirring intensity on the solidification structure is shown in a series of photomicrographs in

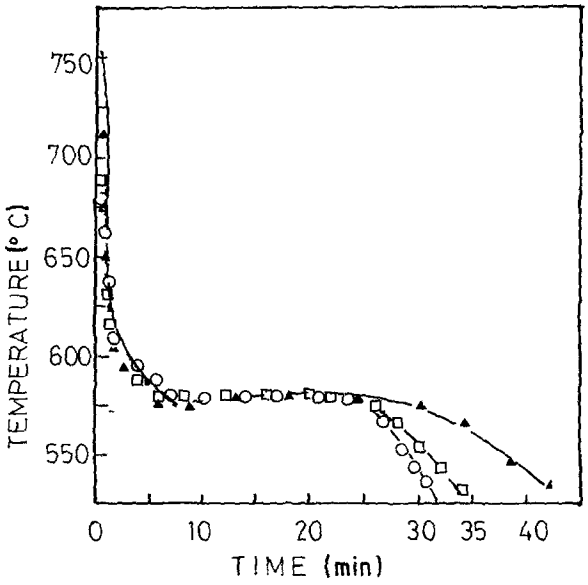

Figure 7 Thermal analysis of electromagnetically stirred hypoeutectic Al–Si alloy ingots at various power levels. Thermocouples were positioned at midradius and 120 mm from the base of a 160 mm high ingot. (○ control, □ 25% full power, ▲ 50% full power)

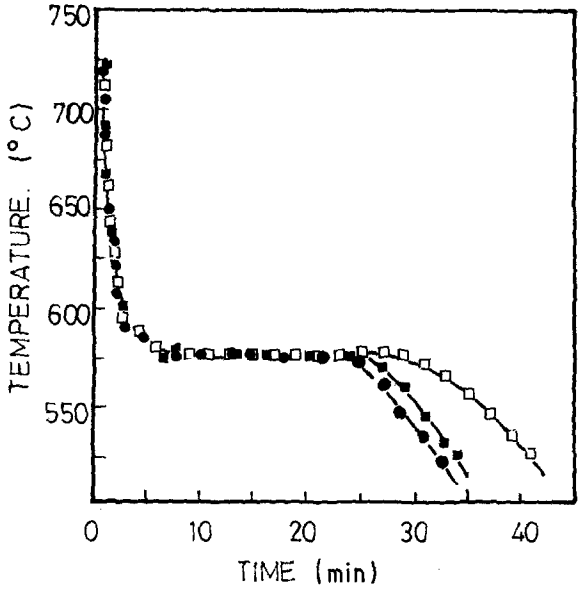

Figure 8 Thermal analysis of the stirred Al–Si alloy ingot with electromagnetic stirring and with mechanical stirring. Thermocouples were positioned at midradius and 80 mm from the base of a 160 mm high ingot. (● control, □ 50% full power 15 min, ■ mechanically stirred 100 r.p.m for 15 min)

Fig. 6. The micrographs show the effect of increasing EMS power levels on the formation of primary aluminium dendrites in the centre of the 550 g hypoeutectic alloy ingots. During normal solidification, columnar growth proceeds with primary aluminium dendrites extending all the way to the centre of the ingot. At low stirring intensities, the primary dendrite arms become detached but the secondary arms are still distinguishable, forming large clusters. As the stirring intensity increases with progressively higher EMS power levels, the cluster size and secondary arm length diminish. At the highest power levels investigated, dendrite fragmentation of growing grains frustrates columnar growth and the thamnitic or bush-like structure is more uniform. The final structure is similar to that obtained in steel with fluid velocities in excess of 25 cm sec^{-1}.

Fig. 7 shows the thermal analysis of hypoeutectic aluminium–silicon alloy ingots cast with EMS at different power levels. The data demonstrates that the final stage of solidification is delayed by EMS and the length of the thermal arrest increases with stirring power. Fig. 8 shows the thermal analysis results which

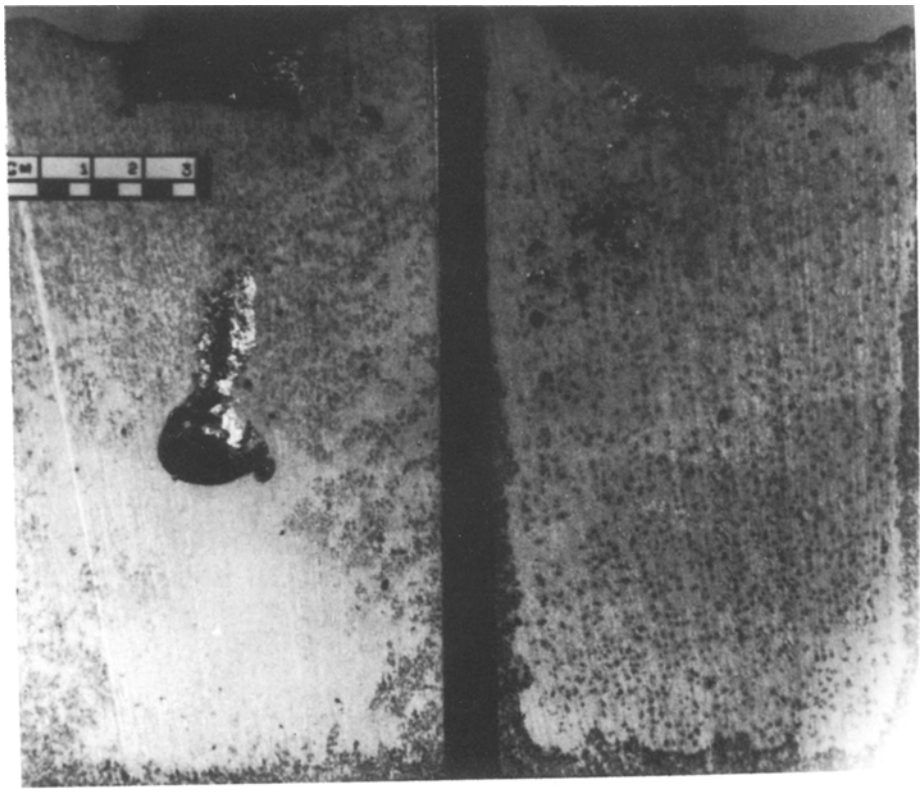

Figure 9 Macrostructure of control and stirred (90% of full power) hypereutectic Al–Si alloys.

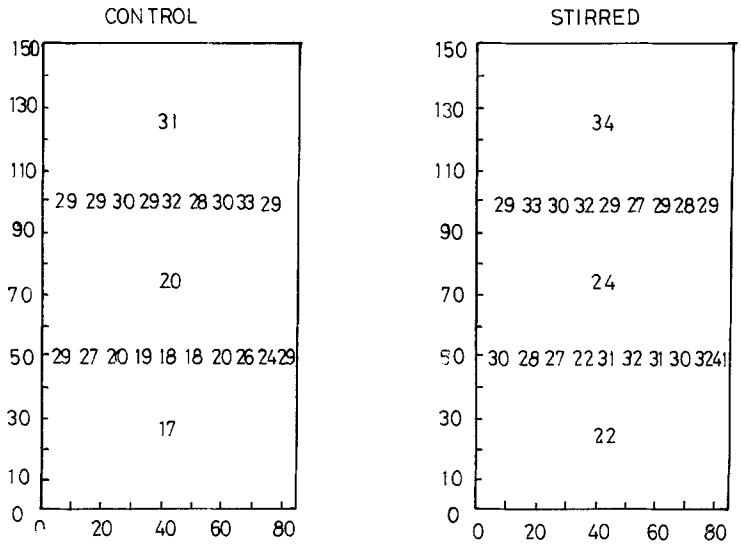

Figure 10 Schematic diagram of the silicon concentration profile in hypereutectic Al–Si alloy ingots.

compare the effect of EMS at 50% of full power and mechanical stirring using a graphite paddle at 100 r.p.m. These results demonstrate that electromagnetic stirring has a more pronounced effect on the thermal arrest than mechanical stirring. This can be attributed to the ability of electromagnetic stirring to penetrate into the interdendritic spaces even after considerable solid has formed. With mechanical stirring this is not possible.

3.3. Studies of hypereutectic aluminium–silicon alloy solidification

Fig. 9 shows the effect of EMS on the macrostructure obtained in 2 kg ingots cast with and without EMS. The control ingot has a large shrinkage cavity in the centre of the ingot and large silicon clusters particularly near the top of the casting. The stirred ingot has a core with less axial porosity, as well as smaller and more uniformly distributed silicon clusters.

Fig. 10 shows the individual silicon determinations across a section of the ingot using atomic absorption analysis for stirred and unstirred ingots. This data was used to plot the concentration profiles as shown in Figs 11 and 12. The plots shows that without stirring, silicon tends to agglomerate and form large clusters which segregate out of the melt by flotation. This results in segregation of silicon, depleting the bottom of the cast ingot of silicon. Stirring with linear EMS appears to inhibit cluster formation and subsequent agglomeration effects. These observations are confirmed in Fig. 13, which shows the results of computer-fitted contour maps. Except for chill effects along the outside edges, the silicon concentration in the stirred ingot is much more uniform in the core of the casting, as compared with the highly segregated control ingot. The effect of stirring intensity on the variation of the silicon concentration is shown in Fig. 14. As the stirring intensity increases, the silicon concentration in the core of the ingot becomes progressively more uniform. At low power levels the silicon segregation was more pronounced, while at high levels the silicon distribution was more homogeneous.

Results from samples taken 50 and 100 mm from the base of the ingot were evaluated by considering the data as two distinct subsets. The first subset consisted of six samples taken from the subsurface region of the casting, while the second subset of five samples was taken from the midradius and core regions of the casting. Statistical analysis of the data, as summarized in Tables I to III, show that a significant amount of silicon segregation occurs in the control ingot. This results in an increase in the silicon concentration of 30.4% between 50 and 100 mm from the base of the control ingot for the core samples. This contrasts with the results obtained with EMS at 90% of full power, which show that the silicon concentration decreased

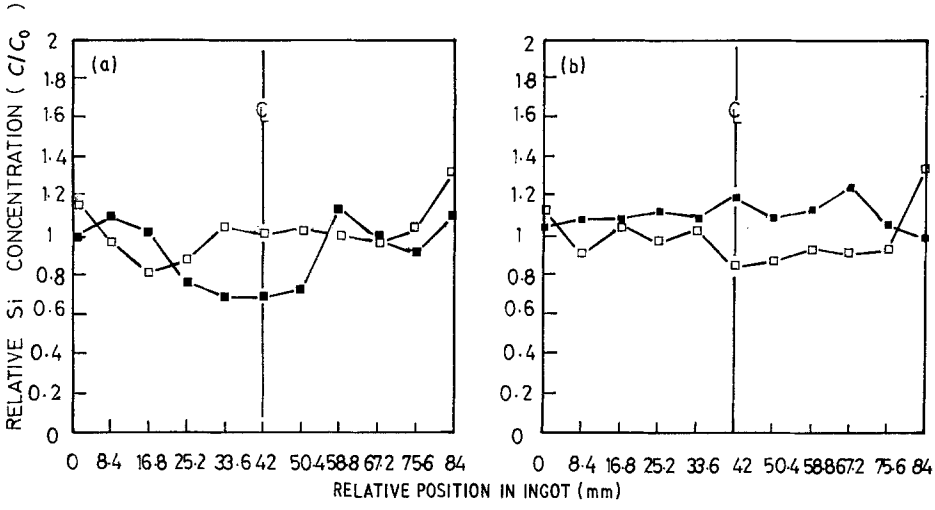

Figure 11 Transverse concentration profiles at 50 mm from the Base (a) and 100 mm from the Base (b) of an ingot showing the effect of EMS (90% of full power) ont the relative silicon concentration in the hypereutectic Al–Si alloy ingots. (■ control, □ stirred)

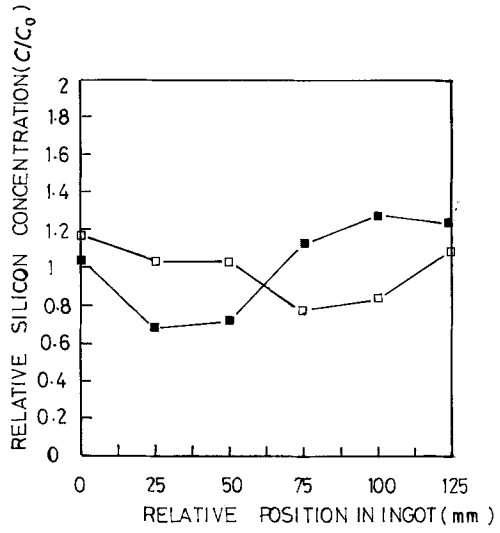

Figure 12 Longitudinal concentration profiles along the ingot centreline showing the effect of EMS (90% of full power) on the relative silicon concentration in the hypereutectic Al–Si alloy ingots. (■ control, □ stirred)

TABLE I Radial segregation of silicon in an aluminium-20 wt % silicon alloy. Drillings were taken 50 mm from the base of the ingot.

Silicon	Average (C/C_0)	Std Dev.	F Calc.	F 0.95	t Calc.	t 0.95
Subsurface (n = 6)						
Control	1.109	0.080				
EMS 30%	1.295	0.445	30.67	6.39	5.45	1.99
EMS 70%	1.080	0.319	15.80	6.39	1.65	1.97
EMS 90%	1.027	0.180	5.01	6.39	0.94	1.81
Core (n = 5)						
Control	0.868	0.211				
EMS 30%	0.646	0.112	3.57	5.05	1.86	1.86
EMS 70%	0.904	0.077	7.54	5.05	3.46	2.01
EMS 90%	0.987	0.067	8.30	5.05	23.4	2.02

by 5.9% in the centre of the ingot. This demonstrates that EMS not only improves the macrostructure of a casting but can also influence the distribution of indigenous particles.

Power levels of 30, 70 and 90% were compared to determine the extent to which the stirring intensity influenced the final silicon distribution 50 mm from the base of the ingot. At the 30% power level, the silicon distribution in the subsurface region appears to be significantly less uniform and more segregated than the control ingot, while the data from the cores of both ingots are very similar. This result indicates that stirring at low power levels can have adverse effects on the mean value and the variability of the silicon distribution. Results at 70% of full power show that the subsurface distribution of silicon is slightly better than the control ingot, while samples from the core of the ingot indicate that both the mean value and variability are improved. However, the best results were obtained at the 90% power level which was the highest power level used. Thus, stirring intensity is an important factor and high power levels are required in order to have a beneficial effect on the segregation pattern produced during the solidification process.

The trials conducted with a linear stirrer met the main objective of providing a useful laboratory-scale simulation of the casting process. The results show both quantitatively and qualitatively how linear EMS affects the cast structure of aluminium–silicon alloys. Computer-fitted models of the data were used to generate contour maps showing the redistribution of silicon clusters with EMS. These studies have yielded new experimental data, which may help to generate a better understanding of both the potential and the limitations of electromagnetic stirring.

4. Conclusions

Data from laboratory testing of a hypoeutectic

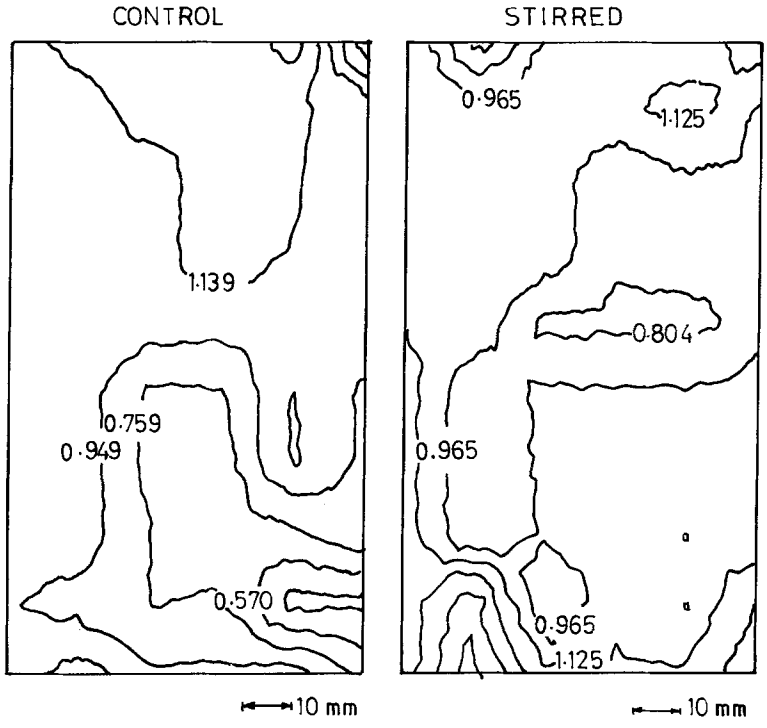

Figure 13 Contour maps showing the effect of EMS (90% of full power) on the variation of the relative silicon concentration in hypereutectic Al–Si alloy ingots.

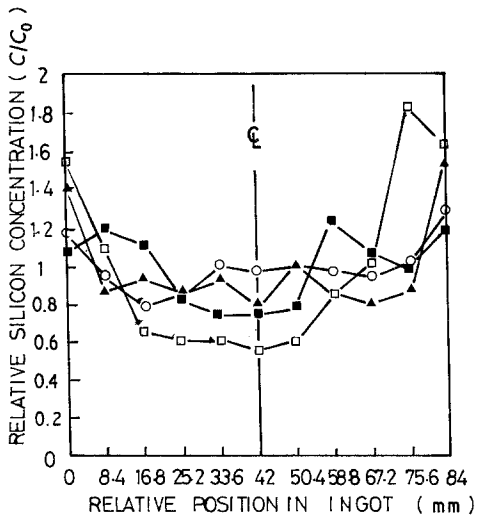

Figure 14 Longitudinal concentration profiles 50 mm from the base of the ingot showing the effect of EMS on the relative silicon concentration in the hypereutectic Al–Si alloy ingots. (■ control, □ 30% full power, ▲ 70% full power, ○ 90% full power)

aluminium–silicon alloy show that continuous linear stirring results in dendrite fragmentation. High stirring intensities, which correspond to high power levels, change the morphology of the cast structure from columnar dendritic to a bush-like thamnitic structure.

In the case of the hypereutectic aluminium–silicon alloy, electromagnetic stirring changes the distribution of the precipitated primary silicon particles. High stirring intensities reduced the amount of silicon segregation throughout the cast structure and produced a sounder core by reducing the axial porosity.

Of the variables tested, electromagnetic stirring power had the most significant effect on the structure of the cast product. Also, it was shown that electromagnetic stirring delayed the solidification process by extending the time of the thermal arrest.

Acknowledgements

The authors would like to thank the Natural Sciences and Engineering Research Council (NSERC) of Canada for the financial support of this work. Also, Dr A. Eastham of the Department of Electrical Engineering at Queen's University is thanked for the provision of the power supply used in this work.

TABLE II Radial segregation of silicon in an aluminium-20 wt % silicon alloy. Drillings were taken 100 mm from the base of the ingot.

Silicon	Average (C/C_0)	Std Dev.	F Calc.	F 0.95	t Calc.	t 0.95
Subsurface (n = 6)						
Control	1.088	0.087				
EMS 90%	1.048	0.176	4.09	6.39	0.45	1.81
Core (n = 5)						
Control	1.132	0.046				
EMS 90%	0.929	0.077	2.73	5.05	4.52	1.86

TABLE III Axial segregation of silicon in aluminium-20 wt % silicon alloy. Drillings were taken along the ingot centreline.

Silicon	Average (C/C_0)	Std Dev.	F Calc.	F 0.95	t Calc.	t 0.95
(n = 6)						
Control	1.013	0.258				
EMS 90%	0.989	0.151	2.92	6.39	0.18	1.81

References

1. K. A. JACKSON, J. D. HUNT, D. R. UHLMANN and T. P. STEWARD, *Trans. Met. Soc. AIME* **236** (1966) 149.
2. W. A. TILLER and S. O. O'HARA, "The solidification of Metals", (Iron and Steel Institute, London, 1967) p. 27.
3. M. H. JOHNSTON and R. A. PARR, *Met. Trans.* **13B** (1982) 35.
4. J. P. GABATHULER and F. WEINBERG, *ibid.* **14B** (1983) 733.
5. A. NISHIMURA, Y. KAWANO and K. FUJITA, *Aluminium* **60** (1984) E512.
6. A. NISHIMURA and Y. KAWANO, *J. Jpn. Inst. Light Met.* **25** (1973) 193.
7. V. A. LIVANOV, V. S. SHIPILOV and R. M. GABIDULLIN, "Light Metal Age" *Metalloved. Term. Obrab. Metal* 6, 2 (1974) p. 8.
8. G. S. REDDY and J. A. SEKHAR, *J. Mater. Sci.* **20** (1985) 3535.

Received 22 October 1987
and accepted 23 February 1988